Colloids and Surfaces A: Physicochem. Eng. Aspects 336 (2009) 88–98

Contents lists available at ScienceDirect

Colloids and Surfaces A: Physicochemical and Engineering Aspects

journal homepage: www.elsevier.com/locate/colsurfa

Dispersion stabilization of conductive transparent oxide nanoparticles

Young-Sang Cho[a,*], Hyang-Mi Kim[a], Jeong-Jin Hong[b], Gi-Ra Yi[c], Sung Hoon Jang[b], Seung-Man Yang[a]

[a] National Creative Research Initiative Center for Integrated Optofluidic Systems and Department of Chemical and Biomolecular Engineering, KAIST, Daejeon 305-701, Republic of Korea
[b] Corporate R&D Center, LG Chem Research Park, Daejeon 305-380, Republic of Korea
[c] Korea Basic Science Institute, Seoul 136-713, Republic of Korea

ARTICLE INFO

Article history:
Received 17 August 2008
Received in revised form 3 November 2008
Accepted 13 November 2008
Available online 21 November 2008

Keywords:
Indium tin oxide
Antimony-doped tin oxide
Nanoparticles
Colloidal stability
Antistatic coatings

ABSTRACT

A colloidal dispersion of indium tin oxide (ITO) nanoparticles in an organic solvent was achieved using a milling process in which β-diketones or titanate coupling agents were used as a dispersing agent. Isopropyl tri(*N*-ethylenediamino)ethyl titanate and 2,4-pentanedione were found to be the most suitable dispersants for stabilizing ITO nanoparticles in a mixed organic solvent. The secondary particle size of the colloidal ITO dispersion was markedly affected by operational parameters in the milling process. Stable dispersions of antimony-doped tin oxide (ATO) nanoparticles in organic solvent, using β-diketones as dispersants, were also prepared. The stable dispersions of ITO and ATO nanoparticles were used as conductive transparent film coatings on cathode-ray tube panels. We found that the electrical conductivity of the film coating was affected by the boiling point of the dispersion stabilizers.

1. Introduction

Indium tin oxide (ITO) has been used as a transparent and conductive film in display applications including electrode, antistatic and electromagnetic interference (EMI) shielding films [1–6]. The shielding of EMI in some display devices has become a particularly important issue because international regulations on EMI have become more restrictive. Moreover, electromagnetic waves can cause critical problems such as malfunctions of electrical machinery and deterioration of the human immune system. The emission of an AC electric field from various video display terminal (VDT) products is regulated by the *Tjänstemännens Centralorganisation* (TCO; the Swedish Confederation of Professional Employees) guidelines [7,8]. Various approaches to addressing these problems have been investigated, including creating thin transparent conductive films on cathode ray tube (CRT) panels using nanoparticles of indium tin oxide (ITO) or antimony-doped tin oxide (ATO) [9]. Although several methods (e.g. chemical vapor deposition, physical vapor deposition, electron beam evaporation, and sputtering) have been developed to deposit ITO films on substrate surfaces, these methods are not adequate for industrial applications as vacuum equipment or high temperature processes are usually required [10]. For continuous production of low cost thin conductive films on display devices, it will be necessary to develop simple and robust wet processes for forming ITO films on substrates using colloidal ITO nanoparticles [11–14].

In preparing coating solutions of ITO nanoparticles, it is essential to stabilize the ITO particles in a mixed organic solvent. In addition, the secondary particle size of the ITO dispersion should be less than 120 nm to prevent strong scattering points from appearing in the film coating. In our experiments the film coating was a double-layered structure with an antistatic (AS) layer derived from the colloidal ITO suspension, and an antireflective (AR) layer of partially hydrolyzed alkyl silicate. The transparent conductive and antireflective films were annealed for solidification and removal of remaining solvent [15]. The optical transparency of the film was enhanced as an overlay AR coating induced destructive interference of incident light onto the CRT panel [16].

For a stable colloidal dispersion of metal oxide nanoparticles, repulsive forces among particles should be strong enough to avoid irreversible aggregation due to van der Waals attraction forces. As the electrostatic repulsive forces of ITO colloids are usually very weak, stabilization is achieved by the adsorption of surfactant molecules on the surface of the colloidal particles, such that the attractive van der Waals interactions are screened [18–23]. This requires selection of a suitable stabilizing agent or surfactant with good dispersion stability for ITO colloids. As titanate coupling agents can form an adsorbed monolayer on the surface of metal oxides, they can be used as a stabilizing agent for the ITO coating

* Corresponding author. Tel.: +82 42 350 3962; fax: +82 42 350 5962.
E-mail address: yscho78@kaist.ac.kr (Y.-S. Cho).

0927-7757/$ – see front matter © 2008 Elsevier B.V. All rights reserved.
doi:10.1016/j.colsurfa.2008.11.014

solution [24]. It is also possible to disperse ITO powder to obtain stable ITO colloids using β-diketones as dispersants, because β-diketones (e.g. 2,4-pentanedione) with bidentate ligands can be adsorbed to the metal oxide surface [25,26].

We report here a simple and easy method for the preparation of stable colloidal ITO or ATO dispersions using β-diketones or coupling agents as dispersants. Various kinds of β-diketones and titanate coupling agents were assessed for suitability as stabilizing agents for nanoparticle dispersion. Some experimental parameters in the milling process were tuned for preparing stable colloidal dispersion from their aggregates, and the effect of composition of the dispersion medium on dispersion stability of the ITO or ATO nanoparticles was also investigated. Multifunctional films on CRT panels were produced using a spin coating process, and their electrical and optical properties were measured.

2. Experimental

2.1. Materials

The ITO and ATO nanopowders were purchased from SinoTech Co. Ltd. (Zhuzhou, China) and Xiamen Zhongli Co. Ltd. (Xiamen City, China), respectively. A mixture of ethanol (Merck, 99.9%), DMF (*N*,*N*-dimethylformamide, Duksan Pharmaceutical Co., 99.9%, Ansan City, Korea), and IPC (2-isopropoxyethanol, Aldrich, 99.9%) was used as the dispersion medium. Titanate coupling agents (Table 1; Kenrich Petrochemicals) were used as dispersion stabilizers for the ITO solution. Other dispersants, 2,4-pentanedione and 3-methyl 2,4-pentanedione, were obtained from Aldrich and Tokyo Kasei Kogyo Co., Ltd. (Osaka, Japan), respectively. ZrO_2 beads (Nanointech, Wonju City, Korea) were used to comminute ITO or ATO powders during the milling process.

2.2. Instrumentation

The morphology of ITO and ATO nanopowders and secondary aggregates of ITO particles were observed by field emission scanning electron microscopy (FE-SEM, Hitachi S4800). The crystalline phases of the ITO and ATO powders were confirmed using X-ray diffraction (XRD) measurements (Rigaku D/MAX-RC). The incident wavelength was Cu Kα = 0.154056 nm and the scan speed was 3°/min. The chemical composition of the ITO and ATO nanopowders was measured using a wavelength dispersive spectrometer (WDS; Electron Probe X-ray Microanalyzer, JXA 8900R) and EDX (Energy Dispersive using X-ray) analysis techniques, respectively. A vibratory paint shaker (Red Devil Equipment Co. Ltd., 5400 series, Y3 model, 670 rpm) was used for the dispersion stabilization and batch milling process for the ITO and ATO solutions, and a Dynomill (KDL A, machine number 000951, Willy Bachofen Maschinefabrik, Basle, Switzerland) was used for continuous milling. The sizes of colloidal ITO and ATO aggregates were characterized by dynamic light scattering (DLS, Zeta Plus, Brookhaven Instruments) at a wavelength of 674 nm and a 90° incident angle. The zeta potential was measured (Zeta Plus) for the sterically-stabilized colloidal ITO dispersion at varying pH values. Nitric acid or potassium hydroxide were used to adjust the pH of the colloidal ITO dispersion. The sheet resistance of the ITO-coated CRT panel was measured using a four probe technique (Loresta HP, MCP-T410, Mitsubishi Chemicals). The visible light reflectance of the film coating was measured using a Darsa Pro-5000 system (Professional Scientific Instruments).

2.3. Dispersion stabilization of ITO and ATO nanoparticles

Colloidal dispersions of ITO particles were prepared by mixing 15 wt% of ITO nanopowder in an organic solvent with dispersants including β-diketones or titanate coupling agents (Table 1). The composition of the dispersion medium was adjusted to 0.67 wt% of dispersant, 74.5 wt% ethanol, 3 wt% DMF, and 7.5 wt% IPC. To disaggregate the ITO powder in organic solvent the milling process with ZrO_2 beads was performed using the paint shaker.

Sedimentation tests were performed for each ITO suspension with the various dispersants (Table 1) to measure the macroscopic stability of the ITO dispersion. Ten milliliter mass cylinders were filled with the colloidal ITO dispersions after they had been comminuted for 8 h. The secondary particle sizes in the ITO dispersions were measured by DLS just prior to the sedimentation test. To avoid evaporation of the organic solvent, the top of the mass cylinder was sealed with rubber and paraffin film. The initial height of each colloidal dispersion in the mass cylinder was measured and compared with the settled height of the ITO aggregates 9 days after sample preparation. The sedimentation ratio of the ITO dispersion was calculated according to Eq. (1), and the results are summarized in Table 1.

$$\text{Sedimentation ratio} = 1 - \frac{\text{settling height of particles}}{\text{initial height of ITO sol}} \quad (1)$$

Stable colloidal dispersions of ATO nanoparticles in ethanol were prepared using β-diketones as dispersants during the milling process with 0.3 mm ZrO_2 beads. The amounts of dispersant and ATO powder in the dispersion media were the same as those used to prepare the ITO dispersions. However, the dispersion medium was pure ethanol and no additional organic solvents were used. The dispersants used to prepare the ATO colloids were 2,4-pentanedione and 3-methyl-2,4-pentanedione.

2.4. Adsorption isotherms of dispersants on the surface of ITO particles

The adsorption isotherms of the dispersants used with the ITO nanoparticles were obtained by elemental analysis (EA, EA1110-FISONS). Dispersants at various concentrations were added to 15 wt% of solid particles in solvent and the mixtures were comminuted for 4 h using the paint shaker. The dispersion medium, ethanol and any excess dispersant were removed from the ITO particles by centrifugation. The remaining ITO particles and adsorbed dispersant were dried in a convection oven at 60 °C, and the elemental composition of the dried ITO powder and dispersant was analyzed by EA to determine the amount of dispersant retained. Specifically, the amount of elemental nitrogen and carbon on the ITO particles was converted to moles of the adsorbed dispersants isopropyl tri(*N*-ethylenediamino)ethyl titanate or 2,4-pentanedione. The surface area of the ITO nanopowder, determined using the BET (Brunauer–Emmet–Teller) method, and the molecular weights of the dispersants were used to calculate the adsorbed moles of dispersant.

2.5. Preparation of the ITO film coating on CRT panels

An ITO film prepared using colloidal ITO nanoparticles was coated onto a 17-inch CRT panel. An antistatic (AS) coating solution was prepared by diluting the ITO suspension (0.9 wt%) stabilized by isopropyl tri(*N*-ethylenediamino)ethyl titanate or 2,4-pentanedione. Before spin coating, the surface of the CRT panel was cleaned with dilute hydrofluoric acid and dried at room temperature under a stream of fresh air. The AS ITO film was overlaid with an AR film by spin coating with a solution of partially hydrolyzed alkyl silicate. The spin coating parameters for the AS and AR films were 140 rpm for 40 s and 160 rpm for 35 s, respectively. The resulting doubled-layered film was annealed at 180 °C for 30 min to ensure complete evaporation of solvent and to enhance the sol–gel reaction of silica precursors, and densification, in the AR overlay.

Table 1
Chemical descriptions of various β-diketones and titanate coupling agents used to disperse nano-sized indium tin oxide particles in organic medium and their results of sedimentation test to disperse indium tin oxide nanoparticles.

Chemical description	ITO (wt.%)	Dispersant (wt.%)	Sedimentation ratio, % (after 9 days)	Secondary particle size of dispersion (nm)	Chemical structure
2,4-pentanedione	15	0.67	0.0	91.3 ± 1.3	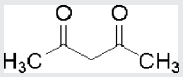
3-methyl 2,4-pentanedione	15	0.67	0.0	101.4 ± 1.2	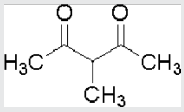
Isopropyl tri(*N*-ethylenediamino)ethyl titanate	15	0.67	0.0	85.1 ± 3.2	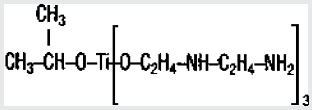
Di(dioctyl pyrophosphate) ethylene titanate	15	0.67	50.5	591.2 ± 11.0	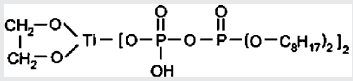
Neopentyl(diallyl)oxy tri(m-amino)phenyl titanate	15	0.67	56.2	744.1 ± 119.0	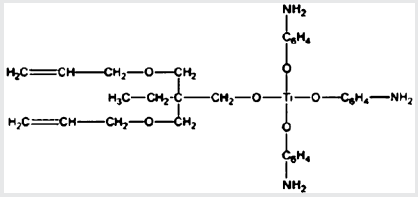
Neopentyl(diallyl)oxy tri(dioctyl)pyro phosphate titanate	15	0.67	56.2	574.7 ± 88.2	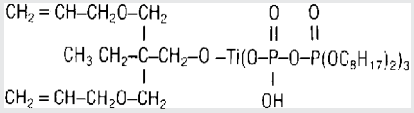

2.6. Sample preparation for electron microscopy

Samples of primary ITO and ATO nanoparticles for EF-TEM (Energy Filtration Transmission Microscopy) imaging were prepared by mixing the ITO or ATO nanopowder with ethanol, followed by ultrasonication. The colloidal ITO or ATO dispersion was then transferred to a standard copper-coated electron microscope grid, and the solvent was evaporated prior to microscopy. The secondary ITO aggregates were prepared by drying dilute, stable suspension of ITO particles on a TEM grid at room temperature prior to examination by EF-TEM.

3. Results and discussion

Most ITO nanoparticles in this study were 20–30 nm in size and spherical or ellipsoidal in shape (Fig. 1a). The ultrafine ATO nanoparticles (about 10 nm in diameter of primary particle size) had an aggregated morphology in a powder state, as shown in Fig. 1b.

Fig. 2a shows the X-ray diffraction pattern of ultrafine ITO powder, which is slightly different from that of pure indium oxide. No diffraction peaks of tin oxide were observed, implying that the ITO powder has a cubic bixbyite crystal structure without any tetragonal crystallites of tin oxide [27]. The primary particle size of ITO

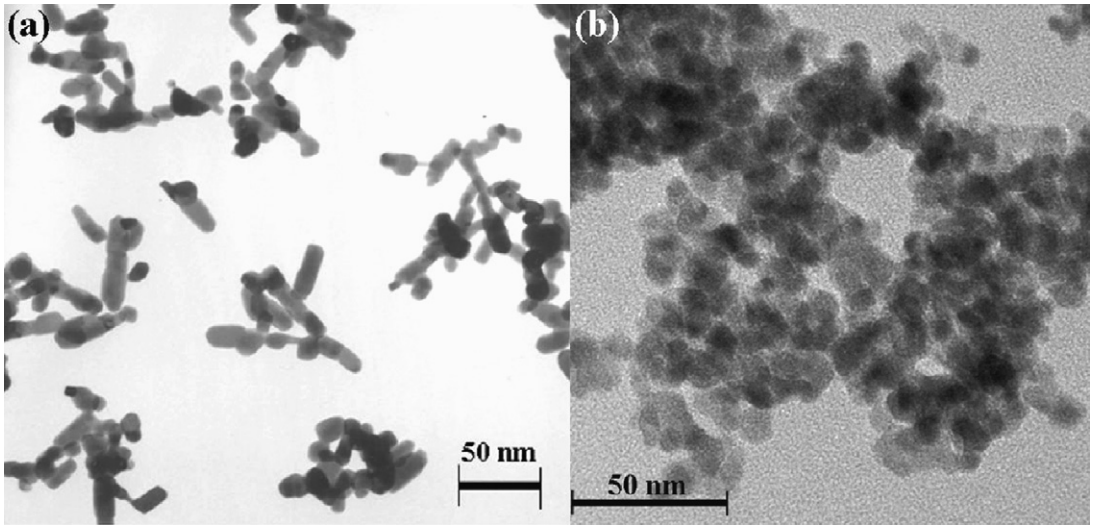

Fig. 1. (a) TEM image of commercialized indium tin oxide powder purchased from SinoTech. Scale bar is 50 nm. (b) TEM image of commercialized antimony-doped tin oxide powder purchased from Xiamen Zhongli Co., Ltd. Scale bar is 100 nm.

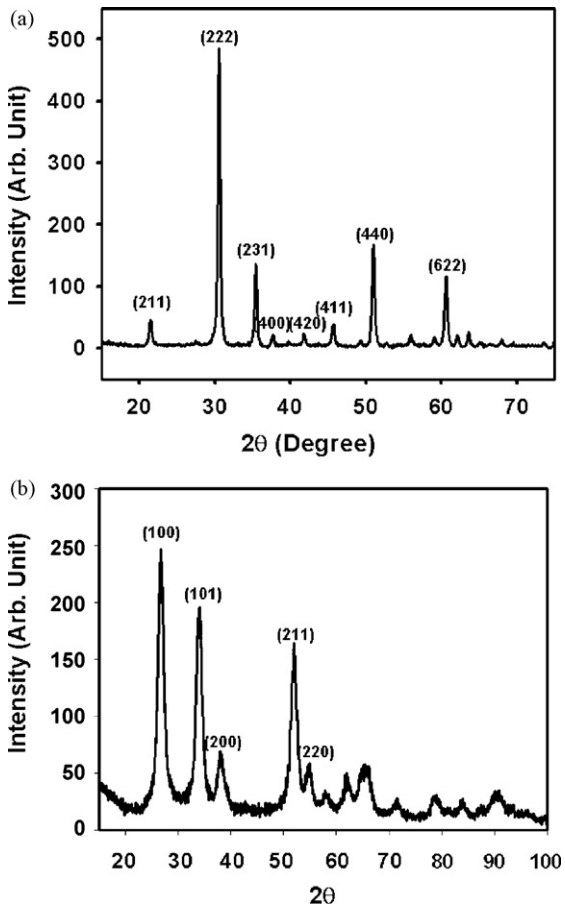

Fig. 2. (a) X-ray diffraction pattern of commercialized ITO powder purchased from SinoTech. (b) X-ray diffraction pattern of commercialized ATO powder purchased from Xiamen Zhongli Co., Ltd.

nanoparticles, calculated using XRD by applying Scherrer's formula, was 22.02 nm [28], which is similar size dimension to that determined from the TEM image in Fig. 1a, although the size and shape of ITO nanoparticles in the image is not monodisperse and irregular. The XRD pattern of ATO nanoparticles (Fig. 2b) shows features characteristic of the SnO_2 tetrahedral structure [29]. The primary particle size of the ATO nanoparticles (9.88 nm), calculated using Scherrer's formula, was comparable size dimension to that based on TEM observations in Fig. 1b, although the exact size of ATO nanoparticles can not be determined upto the level of sub-tenth Angstrom resolution from the image. Thus, we could check the applicability of the Scherrer's formula to compare the theoretical primary particle sizes from X-ray diffraction pattern and the sizes determined from *real* electron micrograph image, and the two approaches showed similar particle size dimensions.

The tin doping ratio, Sn/(Sn + In), of ITO powder used in this study (8.64%) was measured by WDS. As there is a linear increase in the carrier density of ITO up to 8% of the tin doping ratio, and saturation of conductivity occurs at higher tin concentrations, the amount of tin in the ultrafine ITO powder used in this study was optimized for maximum electrical conductivity [30]. The low porosity of the ITO powder, which is essential for high electrical conductivity, was confirmed by measuring the specific surface area and pore volume of ITO particles using the BET method (30.33 m^2/g and 0.214 cm^3/g, respectively). The antimony doping ratio, Sb/(Sb + Sn), of ATO nanoparticles used in this study, measured using the EDX technique, was 12.05%. As the electrical conductivity of ATO saturates when the antimony doping ratio is greater than 10%, it is likely that the amount of antimony in the ATO powder was optimal [31]. The specific surface area of ATO powder was 71.73 m^2/g, according to the manufacturer's data.

Table 1 lists the β-diketones and titanate coupling agents used for preparing colloidal ITO dispersions. Among the β-diketones, 2,4-pentanedione occurs in both the keto and enol forms (the latter, 76%). The greater stability of the enol form can be attributed to resonance stabilization of the conjugated double bonds, and hydrogen bonding. Since hydroxyl groups in the enol form are very reactive [32], adsorption chelation of 2,4-pentanedione to the surface of ITO nanoparticles is possible. Thus, the coordinated compound of β-diketones at the ITO surface may create a steric barrier against van der Waals attraction among particles, resulting in stabilization of the dispersion of colloidal ITO. Titanate or silane coupling agents are also good candidates for stabilization of ITO dispersions, due to chemisorption reactions between the reactive group of the coupling agents and the surface hydroxyl group of the metal oxides of ITO or silica nanoparticles [33,34]. Since the titanate coupling agent such as isopropyl tri(*N*-ethylenediamino)ethyl titanate used in our study has three alkoxy groups, they can react with the surface hydroxyl groups on the ITO nanoparticles. Thus, the adsorption mechanism of titanate coupling agents on the ITO nanoparticles is *chemisorption*. After chemisorption of the coupling agent onto the nanoparticles, the binder functional group of the coupling agent covers the surface of the particles, stabilizing the suspension to an extent dependent on the compatibility of the anchoring functional group with the dispersion medium.

The sizes of secondary ITO particles with various dispersants and their sedimentation test results are summarized in Table 1. The ITO colloidal particles dispersed with β-diketones (2,4-pentanedione and 3-methyl 2,4-pentanedione) or a titanate coupling agent (isopropyl tri(*N*-ethylenediamino)ethyl titanate) did not show an interface between the dispersion medium and particle sediments. Stable ITO dispersions with a green color were observed for these dispersants. However, colloidal ITO powders mixed with the other coupling agents aggregated during the sedimentation test, indicating they had insufficient dispersion capacity [35]. On the basis of the sedimentation tests, the β-diketones and isopropyl tri(*N*-ethylenediamino)ethyl titanate were chosen as the best dispersants for preparing stable colloidal ITO solutions. When 3-methyl 2,4-pentanedione was used as a dispersant the secondary particle size of the ITO dispersion was slightly larger than that of the ITO colloid dispersed with 2,4-pentanedione. This is due to steric interference by the methyl group in chelation of bidentate ligands of 3-methyl 2,4-pentanedione at the surface of the ITO particles. Since the adsorption mechanism of diketones onto the surface of oxide nanoparticles is mainly due to the attachment of chelating groups of diketones with bidentate ligands, the steric hindrance due to the presence of the alkyl chain prevented the diketones from adsorbing with more high efficiency, resulting in the increase of the secondary particle size of colloidal dispersion, when diketones with methyl group such as 3-methyl 2,4-pentanedione was used as dispersants instead of *simple* 2,4-pentanedion.

The adsorption isotherms of isopropyl tri(*N*-ethylenediamino) ethyl titanate and 2,4-pentanedione were obtained for comparison of their adsorption behaviors on the surface of the ITO nanoparticles. Fig. 3a and b shows the adsorption concentrations of isopropyl tri(*N*-ethylenediamino)ethyl titanate and 2,4-pentanedione, respectively, at equilibrium concentrations in the solvent phase. These isotherms are of the Langmuir type, implying strong adsorption behavior at low surface concentration [17]. According to the adsorption isotherm (Fig. 3a), the saturation adsorption concentration of isopropyl tri(*N*-ethylenediamino)ethyl titanate begins at the equilibrium concentration of 7.4 mol/m^3. Based on the weight of ITO powder this corresponds to 2.5 wt% of dispersant. As the amount of dispersant used to prepare the ITO solution was 0.67 wt%, very little dispersant remained

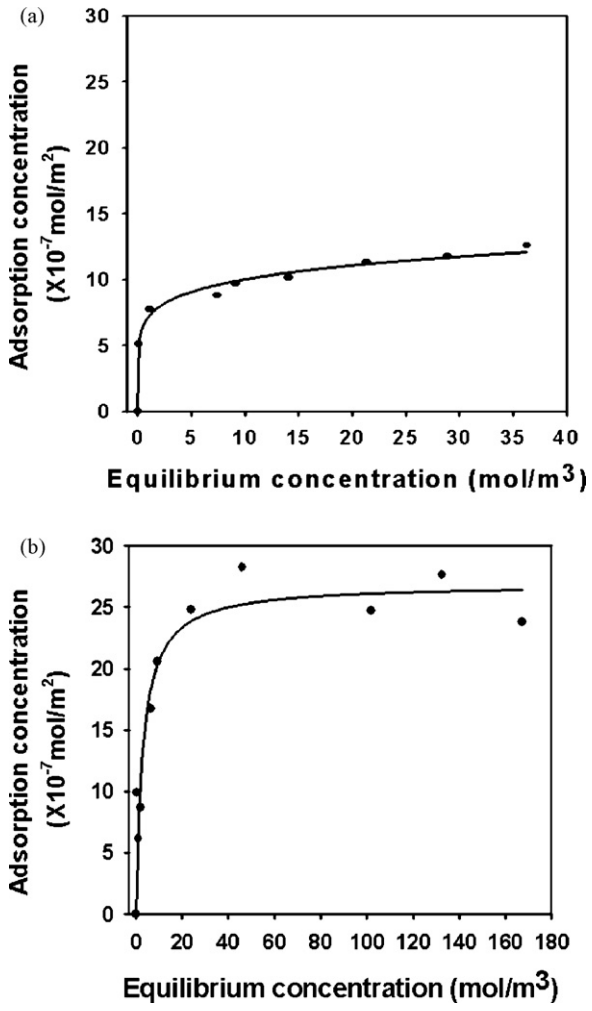

Fig. 3. (a) Adsorption isotherm of tri(*N*-ethylenediamino)ethyl titanate on the surface of indium tin oxide nanoparticles. (b) Adsorption isotherm of 2,4-pentanedion on the surface of indium tin oxide nanoparticles.

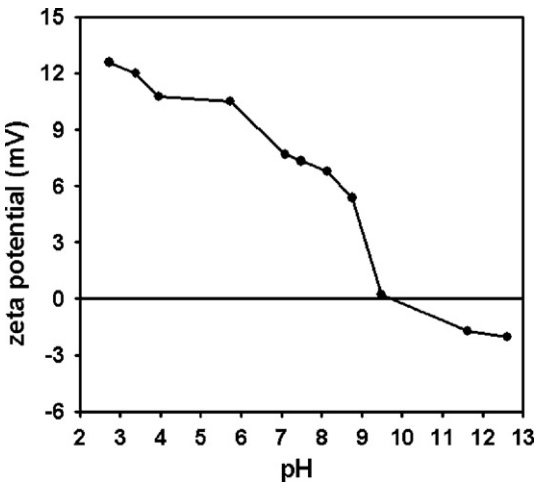

Fig. 4. The zeta potential of colloidal ITO dispersed with tri(*N*-ethylenediamino) ethyl titanate.

in the solvent phase. From the adsorption isotherm of 2,4-pentanedione (Fig. 3b), saturation begins at 9.3 mol/m^3 of the equilibrium concentration. Based on the weight of ITO powder this corresponds to 1.3 wt% of 2,4-pentanedione. The saturated adsorption concentration of 2,4-pentanedione is approximately twice that of isopropyl tri(*N*-ethylenediamino)ethyl titanate, implying that the chemisorption ability of 2,4-pentanedione is greater than that of isopropyl tri(*N*-ethylenediamino)ethyl titanate.

Fig. 4 shows the zeta potential of the sterically stabilized colloidal ITO solution dispersed with isopropyl tri(*N*-ethylenediamino)ethyl titanate at various pH values. As the absolute values of the zeta potential are less than 15 mV, the surface charge of the ITO nanoparticles was almost neutral. Thus, the mechanism of dispersion stabilization by isopropyl tri(*N*-ethylenediamino)ethyl titanate is mainly steric stabilization, and the electrosteric effect can be almost negligible. However, the zeta-potential of ITO nano-colloid stabilized with isopropyl tri(*N*-ethylenediamino)ethyl titanate changes with pH value, implying electrostatic force also contribute to the stabilization of the colloidal suspension, to a certain extent. Usually, the electrostatic stabilization is quite significant especially for the aqueous dispersion of colloidal suspension since the value of zeta potential for this case is several tens of mV. Since our ITO nanoparticles are dispersed in organic medium such as ethanol, the value of zeta potential is too small for electrostatic stabilization. However, we suspect that electrostatic stabilization plays some role for the dispersion stabilization of ITO colloid in this study. From Fig. 4, it is evident that the point of zero charge (PZC) of stabilized ITO particles dispersed with isopropyl tri(*N*-ethylenediamino)ethyl titanate in ethanol ranges from pH 9 to 10. The pH of a stable ITO dispersion without addition of acid or base was about 9.2, and flocculation of ITO particles was observed under both acidic and basic conditions. This may be due to degradation of the anchoring groups of the dispersant on the surface of the ITO nanoparticles, due to the addition of acid or base. We have also tried to measure the zeta potential of *bare* ITO nanoparticles in ethanol as dispersion medium without any dispersant, albeit the measurement was almost impossible since the aggregation of the nanoparticles was too serious since no dispersants were used. However, the measurement of zeta potential will be possible, if the ITO nanoparticles are dispersed in aqueous medium, since electrostatic stabilization mechanism can be applied to this aqueous dispersion. It has been reported that the isoelectric point of ITO nanoparticles in aqueous medium is about 8.5 from theoretical calculation and experimental measurements [36].

For good colloidal stability of ITO dispersions in organic solvents, a milling process in a suitable dispersant is necessary to comminute the aggregated ITO powder by collision energy. In this process the most important factors are the quantity and size of the ZrO_2 beads [37]. Fig. 5a shows the secondary particle size of the ITO dispersion as a function of the size of the ZrO_2 beads following milling of the aggregated ITO powder in solvent in a paint shaker for 8 h. The composition of the ITO dispersion in the sedimentation test was the same for the data shown in Fig. 5a except the diameters of ZrO_2 beads used. Although the same volume of ZrO_2 beads was used to comminute the ITO aggregates, the number of beads increased as the bead diameter decreased. Thus, the collision frequency between the ITO aggregates and the ZrO_2 beads increased as the bead size decreased, and the secondary particle size of the ITO dispersion decreased as the bead size decreased (Fig. 5a). It was impossible to reduce the secondary particle size of the ITO dispersion below 120 nm with ZrO_2 beads larger than 1 mm, even after 8 h of milling.

Fig. 5b shows the secondary particle size of the ITO dispersion as a function of the quantity of ZrO_2 beads (0.3 mm diameter) during batch-type milling in a paint shaker. The collision frequency between the ITO aggregates and the ZrO_2 beads increased as the quantity of beads increased. Thus, the secondary particle size of the ITO dispersion decreased as the bead quantity increased (Fig. 5b). When the quantity of ZrO_2 beads was 1.4 times the weight of the ITO dispersion, the size reduction rate was so slow that it was impos-

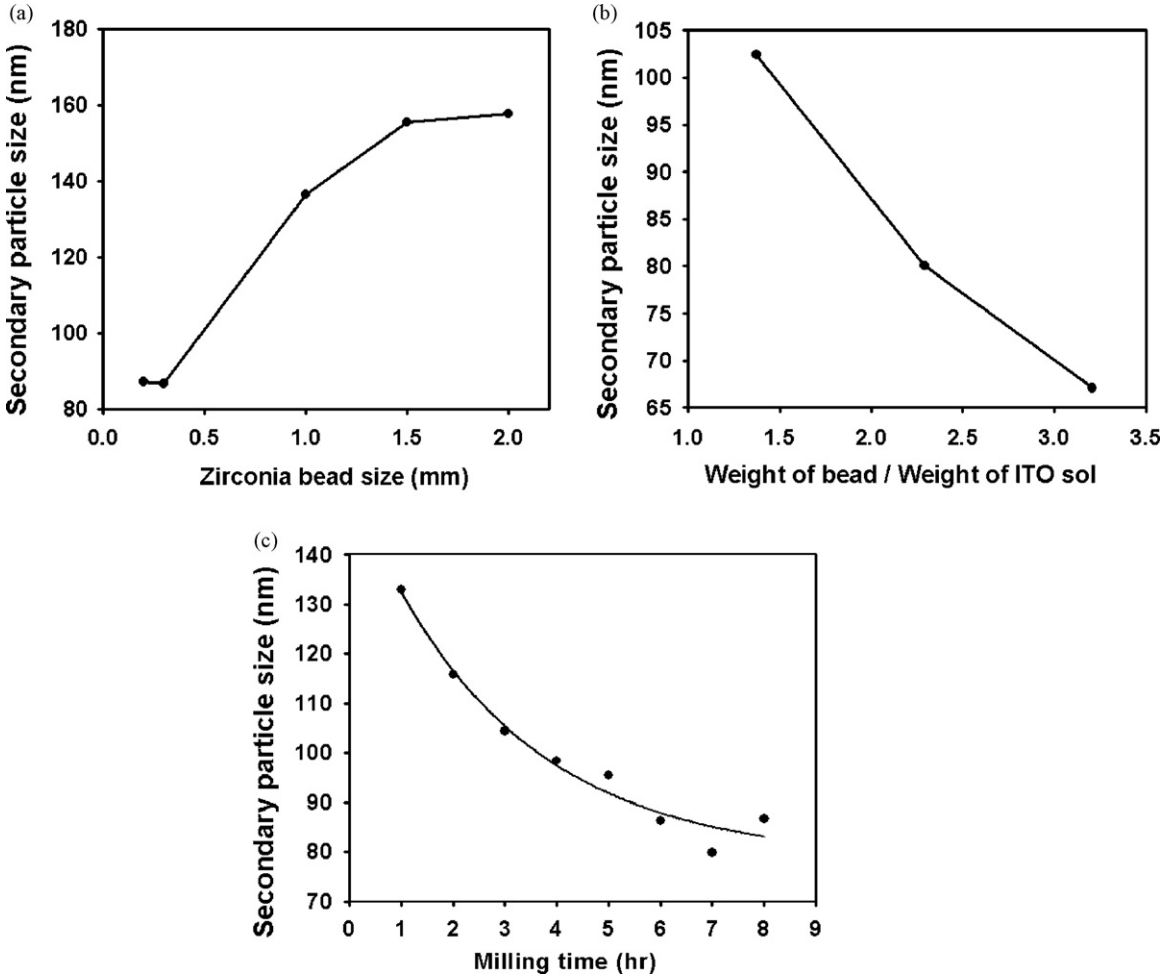

Fig. 5. (a) The secondary particle size of colloidal ITO dispersion as a function of the size of ZrO_2 bead (the attrition duration is 8 h). (b) The secondary particle size of colloidal ITO dispersion as a function of the amount of ZrO_2 bead (the attrition duration is 8 h). (c) The secondary particle size of colloidal ITO dispersion as a function of attrition time (the size of ZrO_2 bead is 0.3 mm and the amount of the bead is 50 ml).

sible to reduce the secondary particle size of the ITO aggregates below 100 nm, even after 8 h of milling. However, when the bead quantity was 3.2 times the weight of the ITO suspension, the aggregate size reduction rate was so fast that the temperature of the ITO dispersion increased markedly during milling. Thus, the optimum quantity of beads was determined to be 2.3 times the weight of the ITO dispersion.

Fig. 5c shows the secondary particle size of the ITO dispersion as a function of milling time (h) when 50 ml of ZrO_2 beads (0.3 mm diameter) was used. Under these optimized operating conditions, the size reduction process seemed to proceed rapidly during the initial milling period, in a similar way to that of metal oxide nanoparticles such as silica nanoparticles during vibration ball milling [38]. However, the aggregate size reduction rate progressively declined, suggesting that a short initial period of milling is the most effective for aggregate size reduction of ITO powder.

Fig. 6a shows a TEM image of secondary aggregates of a colloidal ITO dispersion stabilized with isopropyl tri(*N*-ethylenediamino)ethyl titanate. It is evident from this image that the primary ITO nanoparticles formed very irregular secondary aggregates, and that the number of primary ITO particles comprising each secondary aggregate is not consistent. These irregular aggregates were formed during milling in the paint shaker, where the ITO nanopowders were collided with ZrO_2 beads. Fig. 6b shows a SEM image of the secondary aggregates of the colloidal ITO dispersion. The shape of the ITO aggregates is irregular, and in contrast to the TEM image, it is difficult to identify the primary particles constituting the secondary aggregates. This may be due to the adsorbed coupling agent on the surface of the ITO aggregates. Also important to note is that it is impossible to identify the adsorbed layer of dispersant on the surface of ITO secondary aggregates from TEM image in Fig. 6a due to very small size of the dispersant molecule, isopropyl tri(*N*-ethylenediamino)ethyl titanate. Assuming the chemically adsorbed titanate coupling agents on the surface of ITO nanoparticles are fully extended into the dispersion medium, as depicted in Fig. 6c schematically, we can calculate the thickness of the adsorbed layer of the dispersant accounting the bond length of carbon and other elements such as oxygen and nitrogen in the molecular structure of isopropyl tri(*N*-ethylenediamino)ethyl titanate [39]. The calculated adsorbed layer thickness is about 0.704 to 1.153 nm, which is too short compared with polymeric dispersants for steric stabilization. However, it has been reported that the dense coil conformation of adsorbed polymeric dispersant on the surface of MgO with 1.5–5 nm thickness can act as steric repulsion layer by A. Kauppi [40]. Thus, titanate coupling agent such as isopropyl tri(*N*-ethylenediamino)ethyl titanate can be used as steric stabilizer though the adsorbed layer thickness of the dispersant is relatively short compared with polymeric dispersants. Indeed, other silane coupling agent, MPTS ($(CH_3O)_3Si(CH_2)_3OCOC(CH_3)=CH_2$) has been already used as steric stabilizer for the silica suspension, reflecting titanate coupling agent can be also adopted as dispersant with steric repulsion for ITO nanoparticles [41].

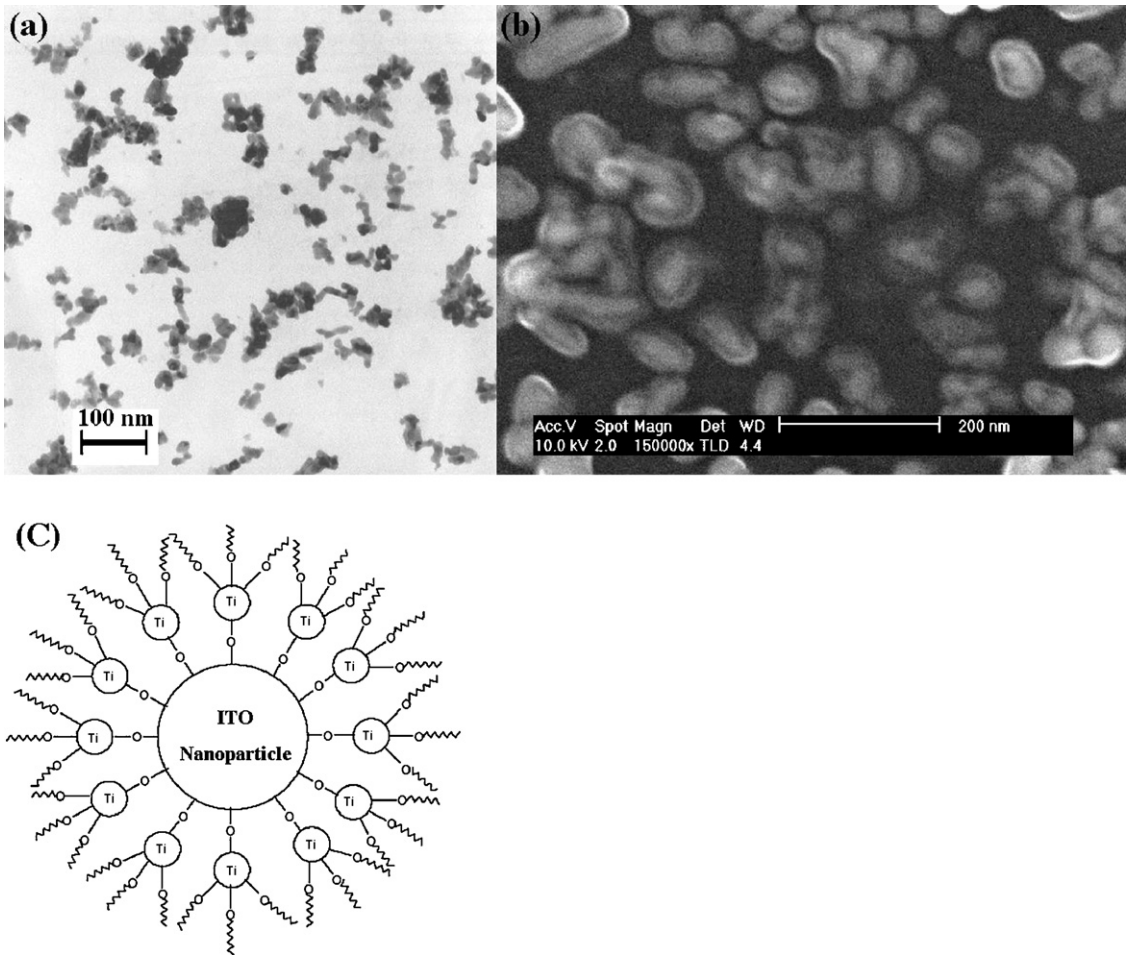

Fig. 6. (a) TEM image of secondary aggregates of ITO colloid. Scale bar is 100 nm. (b) SEM image of secondary aggregates of ITO colloid. Scale bar is 200 nm. (c) Schematic figure for the stabilized ITO nanoparticle adsorbed with titanate modifier.

It is known that the β-diketone 2,4-pentanedione can be adsorbed on the surface of ITO nanoparticles to form a chelate. It has been reported that inorganic condensation between metal oxide nanoparticles occurs when excess ethanol is used as the dispersion medium, as it promotes dehydration of the surface silanol group of the metal oxide nanoparticles, resulting in crosslinking of neighboring particles [42]. This silanol group interparticle inorganic condensation site can be blocked by chelation with β-diketones. In this study it was possible to prepare a stable ITO dispersion when 2,4-pentanedione was adsorbed onto the ITO particle surface. Fig. 7 shows the secondary particle size of colloidal ITO dispersed in 2,4-pentanedione as a function of milling time. 2,4-pentanedione is a less effective dispersant than isopropyl tri(*N*-ethylenediamino)ethyl titanate, due to the very thin adsorption layer thickness of the former compound on the particle surface. This is because the steric repulsion due to 2,4-pentanedione is less than that of isopropyl tri(*N*-ethylenediamino)ethyl titanate. However, when 2,4-pentanedione was used as a dispersant, the secondary particle size of the ITO dispersion was reduced to 114 nm after 4 h of vibratory milling. Fig. 7 also shows the secondary particle size as a function of milling time when a mixture of isopropyl tri(*N*-ethylenediamino)ethyl titanate and 2,4-pentanedione was used as a dispersant. Based on these data it was possible to prepare stable colloidal ITO dispersions after 4 h of vibratory milling when a mixed dispersant is used. These results suggest that neither isopropyl tri(*N*-ethylenediamino)ethyl titanate nor 2,4-pentanedione induces desorption of the other dispersant. A slight increase in secondary particle size in the ITO dispersion was only observed when isopropyl tri(*N*-ethylenediamino)ethyl titanate was used as the dispersant. The heat generated during milling may have caused desorption of isopropyl tri(*N*-ethylenediamino)ethyl titanate, resulting in the increased particle size. This phenomenon was not observed when 2,4-pentanedione was used.

Fig. 8a shows comparative data on the electrical properties, including sheet resistance, of ITO films coated on glass

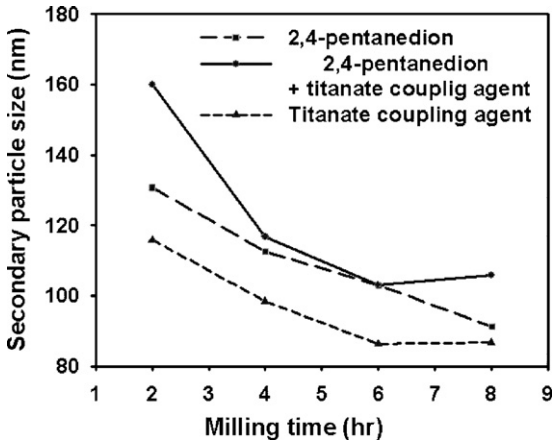

Fig. 7. The secondary particle size of colloidal ITO dispersion as a function of milling time. 2,4-pentanedion, tri(*N*-ethylenediamino)ethyl titanate, and their mixture were used as dispersants.

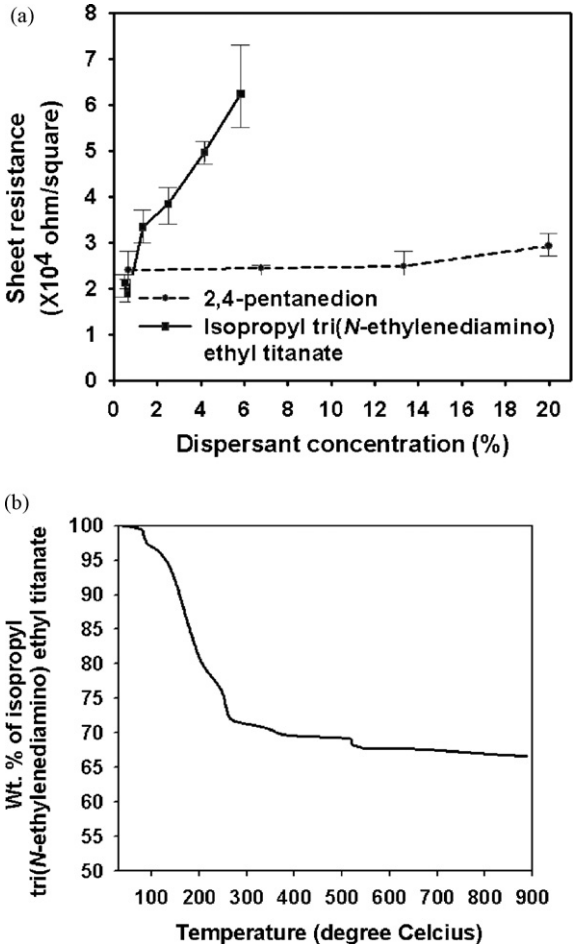

Fig. 8. (a) The sheet resistance of coating film with varying amount of dispersants. (b) The thermogravimetric analysis (TGA) data of isopropyl tri(*N*-ethylenediamino)ethyl titanate.

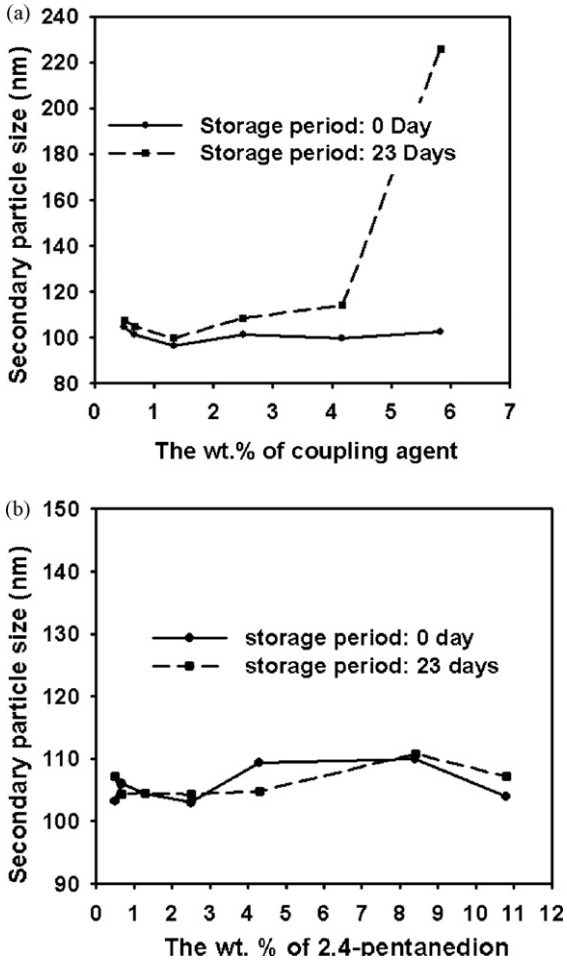

Fig. 9. The change of secondary particle size of colloidal ITO dispersed with 2,4-pentanedion and tri(*N*-ethylenediamino)ethyl titanate as a function of storage day.

with varying amounts of the dispersants such as isopropyl tri(*N*-ethylenediamino)ethyl titanate or 2,4-pentanedione. The secondary particle sizes of colloidal ITO dispersed with isopropyl tri(*N*-ethylenediamino)ethyl titanate and 2,4-pentanedione were adjusted to 101 ± 3.7 and 91.1 ± 1.2 nm, respectively, and the amount of dispersant was based on the weight of ITO powder. According to the thermogravimetric analysis (TGA) shown in Fig. 8b, most of the isopropyl tri(*N*-ethylenediamino)ethyl titanate was retained, and acted as an insulating layer after baking of the coating at 180 °C [35]. However, the 2,4-pentanedione evaporated completely after baking, as the boiling point of 2,4-pentanedione (140 °C) is low enough to cause vaporization during the baking process. Thus, the adsorption layer of 2,4-pentanedione between the ITO aggregates in the baked film will not remain, and the electrical resistance due to the adsorbed dispersant layer will be non-existent. The sheet resistance of the ITO coating was almost independent on the amount of 2,4-pentanedione as displayed in Fig. 8(a). In contrast, the electrical resistance of the film increased markedly with increasing isopropyl tri(*N*-ethylenediamino)ethyl titanate. The measured sheet resistance of the film ranged from 2.4 to $3.0 \times 10^4\ \Omega/\square$, which is sufficient to shield the CRT panel from electromagnetic waves, and satisfies semi-TCO regulations.

The long-term stability of a colloidal dispersion is important, as aggregation of particles in the dispersion medium will affect the physical properties of the dispersion and its engineering applications. To study the dispersion stability of ITO nanoparticles as a function of storage time, we measured and compared the secondary particle sizes of the colloids dispersed with isopropyl tri(*N*-ethylenediamino)ethyl titanate and 2,4-pentanedione, and stored at 4 °C for 23 days (Fig. 9). For tri(*N*-ethylenediamino)ethyl titanate (Fig. 9a) the secondary particle size increased less than 15 nm when the dispersant concentration was less than 4.2 wt%, but increased by a factor of about two when 5.8 wt% of dispersant was used. This may be due to depletion interaction due to unadsorbed dispersant dissolved in the dispersion medium, causing an attractive osmotic pressure and resulting in particle aggregation [35,43]. Thus, the critical concentration for depletion flocculation lies between 4.2 and 5.8 wt% of isopropyl tri(*N*-ethylenediamino)ethyl titanate; this finding suggests that an adequate amount of the coupling agent should be used to guarantee the long-term stability of the colloidal ITO dispersion. This is the manifestation of the existence of optimum concentration of dispersant for stable ITO dispersion when titanate coupling agent was used as dispersion stabilizer.

Fig. 9b shows that after 23 days there was a slight change in the secondary particle size in an ITO dispersion stabilized by 2,4-pentanedione varying from 0.5 to 10.8 wt%, indicating that the secondary particle size remained almost constant regardless of the concentration of dispersant. Since 2,4-pentanedione is a small molecule, similar in molecular size to the solvents in the dispersion medium, the depletion layer does not occur on the surface of ITO particles when 2,4-pentanedione is used as the dispersant. Consequently, no change was observed in the particle size in ITO dispersions due to depletion flocculation. This suggests that if 2,4-pentanedione is used, ITO dispersions will remain stable for long storage times regardless of the amount of dispersant used.

Thus far, the dispersion stabilization of ultrafine ITO powder in a batch type vibratory milling apparatus has been described as a function of various operational parameters. However, continuous operation of the powder milling process is essential for industrial applications. We therefore used a continuous operation milling machine, the Dynomill, which uses an agitation disk to comminute the aggregated nanopowder with ZrO_2 beads, i.e., it functions as an agitator bead mill. A mixture of ITO powder, dispersion medium and the dispersant isopropyl tri(*N*-ethylenediamino)ethyl titanate, with the same composition as that used in the batch experiments, was fed into the Dynomill chamber and agitated with 230 ml of ZrO_2 beads at 2667 rpm. The feed rate was adjusted to 10.3 L/h, and the ITO suspension from the mill outlet was recycled for several hours and sampled at various times during the continuous milling process. It was found that the secondary particle size of the ITO suspension could be reduced to less than 124.1 nm (Fig. 10a), and the electrical conductivity of coating film with this AS coating was $3.7 \times 10^4\ \Omega/\square$. Fig. 10b shows the reflectance spectrum of visible light for the AS and AR coating layers on the CRT panel. Before deposition of the AS coating solution, the ITO colloids were dispersed with isopropyl tri(*N*-ethylenediamino)ethyl titanate in the Dynomill. The minimum reflectance of the film coating was 1–1.5%,

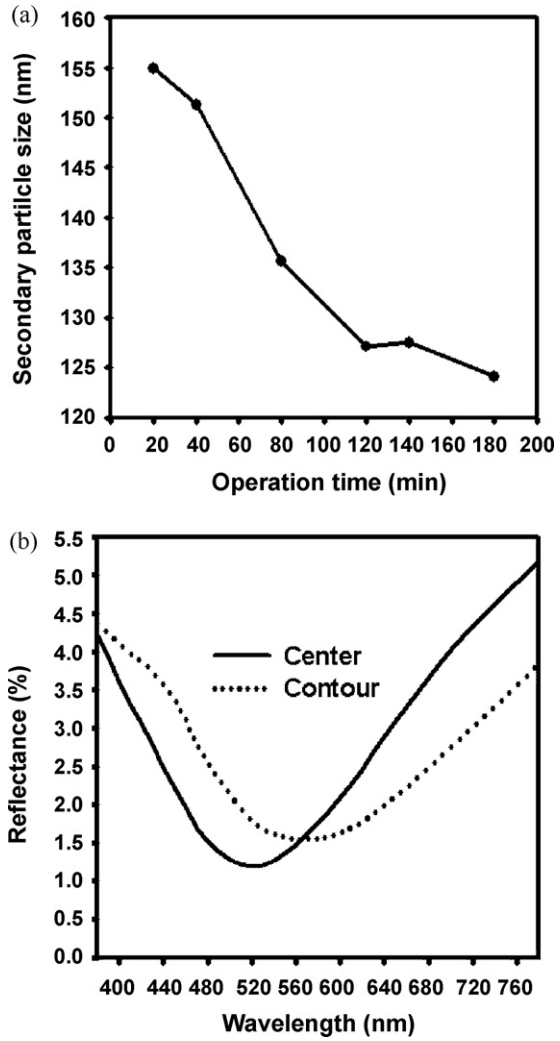

Fig. 10. (a) The secondary particle size of ITO dispersion during continuous milling process by Dynomill. Isopropyl tri(*N*-ethylenediamino)ethyl titanate or 2, 4-pentaneion was used as dispersant. (b) The reflectance spectrum of coating film. Isopropyl tri(*N*-ethylenediamino)ethyl titanate or 2,4-pentanedion was used as dispersant for continuous milling process by Dynomill.

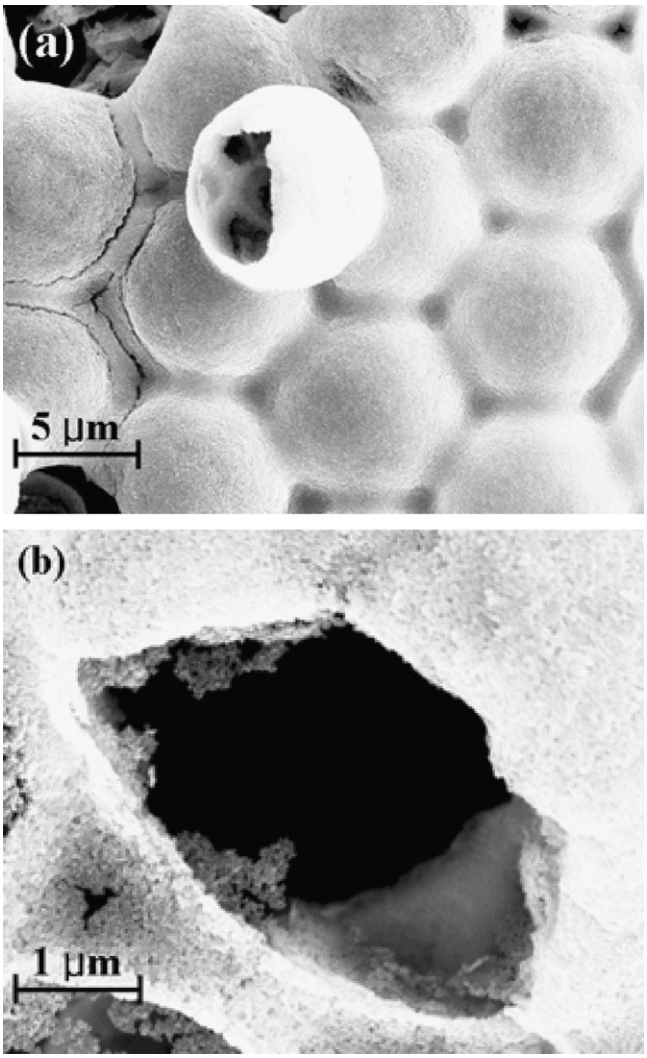

Fig. 11. (a) SEM image of hollow microsphere array made of indium tin oxide nanoparticles, (b) high magnification image of the same sample.

depending on the measurement position, and the coating surface was clean without whitening of the film.

The diluted suspension (0.5 wt%) of ITO nanoparticles dispersed with 2,4-pentanedione was infiltrated into a hexagonal array of polystyrene (PS) microspheres (10.1 μm in diameter; Duke Scientific Co. Ltd.) to obtain conductive macroporous films by using hetero-coagulation of ITO nanoparticles and PS microspheres in mixed suspension [44]. After complete infiltration and drying the sample was heated at 500 °C to remove organic PS microspheres, leaving hollow microsphere arrays made of ITO nanoparticles as shown in Fig. 11a. High magnification SEM image in Fig. 11b revealed ITO nanoparticles comprising the walls of the conductive hollow structures, implying that the dispersion stability of the ITO solution was retained during the colloidal templating process. The macroporous ordered arrays of ITO has important applications such as porous electrodes for photoelectrochemical cells. This application has been already accomplished by sputtering ITO on the polystyrene opal by other group [45]. As an alternative approach, we have used ITO nanoparticle suspension to be infiltrated into the PS opal array as described in our manuscript.

Fig. 12 shows the secondary particle size of the ATO colloid dispersed in ethanol. As shown in Fig. 11, the secondary particle size in the ATO solution dispersed in 2,4-pentanedione was smaller than that in the ATO solution stabilized with 3-methyl-2,4-

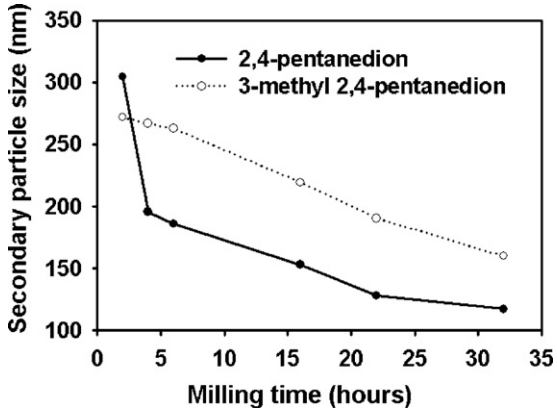

Fig. 12. The change of secondary particle size of colloidal ATO dispersed with 2,4-pentanedion and 3-methyl-2,4-pentanedione as a function of attrition time.

pentanedione (milling time 32 h), suggesting that steric hindrance due to the methyl group of 3-methyl-2,4-pentanedione prevented the preferred adsorption of the dispersant onto the surface of ATO aggregates relative to 2,4-pentanedione. The milling time required to achieve a stable ATO colloid was longer than that for ITO nanoparticles, indicating that it is difficult to comminute aggregated ATO nanoparticles of relatively small primary particle size (9.88 nm) by the milling process.

4. Conclusions

A colloidal ITO dispersion was prepared by milling of ultrafine ITO powder using β-diketones (including 2,4-pentanedione) or titanate coupling agents (including isopropyl tri(*N*-ethylenediamino)ethyl titanate) as dispersants. The adsorption behavior of both types of dispersant on the surfaces of the ITO particles was studied. The saturated adsorption concentration of 2,4-pentandion was twice that of isopropyl tri(*N*-ethylenediamino)ethyl titanate, implying that β-diketones have a stronger affinity for the ITO surface than does the titanate coupling agent. Under the same milling conditions the colloidal ITO dispersion stabilized with isopropyl tri(*N*-ethylenediamino)ethyl titanate had secondary particles of smaller size than the ITO dispersion stabilized with 2,4-pentanedione. This occurred because the adsorbed layer of the coupling agent, which acts as a steric barrier blocking van der Waals interactions on the surfaces of ITO nanoparticles, was thicker than that of the β-diketone layer.

The colloidal ITO dispersion was deposited on the CRT panel to increase its surface conductivity, and partially hydrolyzed alkyl silicate was overlaid onto the ITO coating. The sheet resistance of this double-layered film increased in proportion to the amount of isopropyl tri(*N*-ethylenediamino)ethyl titanate, as the adsorbed coupling agent acts as an insulating layer between the ITO nanoparticles. The sheet resistance of the film coating was independent of the amount of 2,4-pentanedione used, due to evaporation of the dispersant during baking of the film.

The colloidal ITO dispersion stabilized with the coupling agent showed depletion flocculation when the concentration of dispersant was greater than 4.2 wt%. In contrast, the ITO solution dispersed by β-diketone did not flocculate over the wide range of dispersant concentrations used, as 2,4-pentanedione did not create a depletion layer on the surface of the ITO nanoparticles. The stability of the ITO dispersion was retained during the colloidal templating process, forming conductive hollow microsphere arrays.

Colloidal ATO dispersions stabilized with β-diketones including 2,4-pentanedione and 3-methyl-2,4-pentanedione were also prepared using a paint shaker to make a conductive paste dispersed in an organic solvent such as ethanol.

Acknowledgments

This work was supported by a grant from the Creative Research Initiative Program of the Ministry of Science & Technology for "Complementary Hybridization of Optical and Fluidic Devices for Integrated Optofluidic Systems." Dr. Gi-Ra Yi was supported by KBSI grant (N28073). The authors also acknowledge the Korea Basic Science Institute for the transmission electron microscopy.

References

[1] Y. Djaoued, V.H. Phong, S. Badile, Sol-gel prepared ITO films for electrochromic systems, Thin Solid Films 293 (1997) 108–112.
[2] G. Kawachi, E. Kimura, Y. Wakui, N. Konoshi, H. Yamamoto, Y. Matsukawa, A. Sasano, A novel technology for a-Si TFT-LCD's with buried ITO electrode structure, IEEE T. Electron. Dev. 41 (7) (1994) 1120–1124.
[3] P. Stulik, J. Singh, Study of the effect of introducing a bottom ITO layer in an a-Si:H p-i-n type solar cell, Sol. Energ. Mat. Sol. C. 40 (3) (1996) 239–251.
[4] K. Molnar, T. Mohacsy, P. Varga, E. Vazsonyi, I. Barsony, Characterization of ITO/porous silicon LED structures, J. Lumin. 80 (1999) 91–97.
[5] J.S. Kim, R.H. Friend, F. Cacialli, Surface wetting properties of treated indium tin oxide anodes for polymer light-emitting diodes, Synthetic Metals 111–112 (2000) 369–372.
[6] S.K. Park, J.I. Han, W.K. Kim, M.G. Kwak, Deposition of indium-tin-oxide films on polymer substrates for application in plastic-based flat panel displays, Thin Solid Films 397 (2001) 49–55.
[7] Institute of Electrical and Electronic Engineers, IEEE C95.1-1991, IEEE standards for safety levels with respect to human exposure to radio frequency electromagnetic fields, 3 kHz to 300 GHz, New York, 1992.
[8] P.E. Bovie, Global standard – how computer displays worldwide got the TCO logo, 1st ed., Premiss Forlag, 2007.
[9] R.G. Gordon, Criteria for choosing transparent conductors, MRS Bull. 25 (8) (2000) 52–57.
[10] A.L. Dawar, J.C. Joshi, Semiconducting transparent thin films, J. Mater. Sci. 19 (1984) 1–23.
[11] D.M. Mattox, Sol-gel derived, air-baked indium and tin oxide films, Thin Solid Films 204 (1991) 25–32.
[12] J.J. Xu, A.S. Shaikh, R.W. Vest, Indium tin oxide films from metallo-organic precursors, Thin Solid Films 161 (1988) 273–280.
[13] Y. Takahashi, S. Okada, R.B.H. Tahar, K. Nakano, T. Ban, Y. Ohya, Dip-coating of ITO films, J. Non-cryst. Solids 218 (1997) 129–134.
[14] M. Toki, M. Aizawa, Sol-gel formation of ITO thin film from a sol including ITO powder, J. Sol-gel Sci. Technol. 8 (1997) 717–720.
[15] A. Toufuku, K. Adachi, U. S. Patent no. 5,785,897, 28 Jul. 1998.
[16] T. Morimoto, Y. Sanada, H. Tomonaga, Wet chemical functional coatings for automotive glasses and cathode ray tubes, Thin Solid Films 392 (2001) 214–222.
[17] D.J. Kim, H. Kim, Dependence of the rheological behavior of electrostatically stabilized alumina slurries on pH and solid loading, J. Mater. Sci. 33 (1998) 2931–2935.
[18] L. Wang, W. Sigmund, F. Aldinger, Systemic approach for dispersion of silicon nitride powder in organic media: II, dispersion of the powder, J. Am. Ceram. Soc. 83 (4) (2000) 697–702.
[19] P. Somasundaran, D.W. Fuerstenau, Mechanisms of alkyl sulfonate adsorption at the alumina-water interface, J. Phys. Chem. 70 (1966) 90–96.
[20] K. Esumi, A. Sugimura, T. Yasmada, K. Meguro, Adsorption of dioctadecyldimethylammonium chloride on silica, Colloids Surf. 62 (1992) 249–254.
[21] M.S. Celik, R.H. Yoon, Adsorption of poly(oxyethylene)nonylphenol homologs on a low ash coal, Langmuir 7 (1991) 1770–1774.
[22] Y. Ihara, Adsorption of anionic surfactants and related compounds from aqueous solution onto activated carbon and synthetic adsorbent, J. Appl. Polym. Sci. 44 (1992) 1837–1840.
[23] D.H. Napper, J. Steric Stabilization, Colloid Interface Sci. 58 (1977) 390–407.
[24] H. Takeda, Y. Ohtsuka, K. Adachi, H. Kuno, Coating solution for a heat-ray shielding film and a process for forming a heat-ray shielding film by employing the same, US Patent no. 5,840,364, 24 Nov. 1998.
[25] V. Peyre, O. Spalla, L. Belloni, Compressoin and reswelling of nanometric zirconia dispersions: effect of surface complexants, J. Am. Ceram. Soc. 82 (5) (1999) 1121–1128.
[26] J.-J. Hong, S. H. Jang, S.-M. Yang, Y.-S. Cho, The conductive metal oxides dispersion using β-diketone as a dispersant and the anti-static, conductive coating layer for using the same, Korean Patent no. 10-0727760, 13 Jun. 2007.
[27] Z. Gao, Y. Gao, Y. Li, Y. Li, Effect of heat treatments on the microstrucure of nanophase indium tin oxide, Nanostructured Mater. 11 (5) (1999) 611–616.
[28] B.D. Cullity, Elements of X-ray Diffraction, 3rd ed., Prentice Hall, 2001.
[29] H.-J. Jeon, M.-K. Jeon, M. Kang, S.-G. Lee, Y.-L. Lee, Y.-K. Hong, B.-H. Choi, Synthesis and characterization of antimony-doped tin oxide (ATO) with nanometer-sized particles and their conductivities, Mater. Lett. 59 (2005) 1801–1810.

[30] N. Yamada, I. Yasui, Y. Shigesato, H. Li, Y. Ujihira, K. Nomura, Doping mechanisms of Sn in In_2O_3 powder studied using ^{119}Sn Mossbauer spectroscopy and X-ray diffraction, Jpn. J. Appl. Phys. 38 (1999) 2856–2862.
[31] T.-Y. Lim, C.-Y. Kim, B.-S. Kim, B.G. Choi, K. Shim, Effect of N_2 gas annealing and SiO_2 barrier on the optical transmittance and electrical resistivity of a transparent Sb-doped SnO_2 conducting film, J. Mater. Sci. Mater. El. 16 (2005) 71–76.
[32] P.A. Cornnor, K.D. Dobson, A.J. McQuillan, New sol-gel attenuated total reflection infrared spectroscopic method for analysis of adsorption at metal oxide surfaces in aqueous solutions. Chelation of TiO_2, ZrO_2, and Al_2O_3, surfaces by catechol, 8-quinolinol, and acetylacetone, Langmuir 11 (1995) 4193–4195.
[33] C.A. Wah, L.Y. Choong, G.S. Neon, Effects of titanate coupling agents on rheological behavior, dispersion characteristics and mechanical properties of talc filled polypropylene, Eur. Polym. J. 36 (2000) 789–801.
[34] M. Iiijima, M. Tsukada, H. Kamiya, Effect of the particle size on surface modification of silica nanoparticles by using silane coupling agents and their dispersion stability in methylethylketone, J. Colloid Interf. Sci. 307 (2007) 418–424.
[35] Y.-S. Cho, G.-R. Yi, J.-J. Hong, S.H. Jang, S.-M. Yang, Colloidal indium tin oxide nanoparticles for transparent and conductive films, Thin Solid Films 515 (2006) 1864–1871.
[36] J. Sun, B.V. Velamakanni, W.W. Gerberich, L.F. Francis, Aqueous latex/ceramic nanoparticles dispersions: colloidal stability and coating properties, J. Colloid Interface Sci. 280 (2004) 387–399.
[37] D.W. Fuerstenau, J.J. Lutch, A. De, The effect of ball size on the energy efficiency of hybrid high-pressure roll mill/ball mill grinding, Powder Technol. 105 (1999) 199–204.
[38] Y. Kanno, Properties of SiC, Si_3N_4, and SiO_2 ceramic powders produced by vibratoin ball milling, Powder Technol. 44 (1985) 93–97.
[39] R.C. Weast, Handbook of Chemistry and Physics, 65th ed., CRC Press, Inc., 1985.
[40] A. Kauppi, K.M. Andersson, L. Bergstrom, Probing the effect of superplasticizer adsorption on the surface forces using the colloidal probe AFM technique, Cement Concrete Res. 35 (2005) 133–140.
[41] J.-H. So, S.-M. Yang, C. Kim, J.C. Hyun, Microstructure and rheological behavior of electrosterically stabilized silica particle suspensions, Colloids Surf. A 190 (2001) 89–98.
[42] S. Allison, Analysis of the electrophoretic mobility and viscosity of dilute Ludox solutions in terms of a spherical gel layer model, J. Colloid Interface Sci. 277 (2004) 248–254.
[43] W.B. Russel, D.A. Saville, W.R. Showalter, Colloidal Dispersion, Cambridge University Press, New York, 1999, p. 189.
[44] Y. Sakka, F. Tang, H. Fudouzi, T. Uchikoshi, Fabrication of porous ceramics with controlled pore size by colloidal processing, Sci. Tech. Adv. Mater. 6 (2005) 915–920.
[45] L. Yang, Novel nanostructured electrodes, PhD Thesis, Department of Chemistry, University of Wollongong, 2007.